Title

Improvement in Oxidation Behavior of Nanostructured CoNiCrA1Y Bond Coat Dispersed with Nano-size Alumina Particles

Authors

Tang, Feng
Ajdelsztajn, Leonardo
Kim, Geoge E.
et al.

Publication Date

2002-12-02

Fundamental Science of Energy 004

"IMPROVEMENT IN OXIDATION BEHAVIOR OF NANOSTRUCTURED CoNiCrA1Y BOND COAT DISPERSED WITH NANO-SIZE ALUMINA PARTICLES"

Feng Tang, Leonardo Ajdelsztajn, Geoge E. Kim, Virgil Provenzano and Julie M. Schoenung

December 2002

This paper is part of the University of California Energy Institute's (UCEI) Energy Policy and Economics Working Paper Series. UCEI is a multi-campus research unit of the University of California located on the Berkeley campus.

UC Energy Institute
2539 Channing Way, # 5180
Berkeley, California 94720-5180
www.ucei.org

Synthesis and Oxidation Behavior of Nanocrystalline MCrAlY Bond Coats

Leonardo Ajdelsztajn[a], Feng Tang[a], Josep Picas[b], Geoge E. Kim[c], Virgil Provenzano[d] and Julie M. Schoenung[a]

[a]Department of Chemical Eng. and Materials Science, University of California, Davis, CA 95616
[b]Depart. Ciencia de Materials i Eng. Metallurgica, Universitat Politecnica de Catalunya, Vilanova i la Geltru, 08800, Spain.
[c]Perpetual Technologies, Montreal, Quebec, Canada H3E 1T8
[d]National Institute of Standards and Technology, Gaithersburg, MD 20899

Abstract

Thermal barrier coating (TBC) systems protect turbine blades against high-temperature corrosion and oxidation. They consist of a metal bond coat (MCrAlY, M = Ni, Co) and a ceramic top layer (ZrO_2/Y_2O_3). In this work the oxidation behavior of conventional and nanostructured HVOF NiCrAlY coatings has been compared. Commercially available NiCrAlY powder was mechanically cryomilled and HVOF sprayed on a nickel alloy foil to form a nanocrystalline coating. Free-standing bodies of conventional and nanostructured HVOF NiCrAlY coatings were oxidized at a 1000°C for different time periods in order to form the thermally grown oxide (TGO) layer. The experiments show an improvement in oxidation resistance in the nanostructured coating when compared to that of the conventional one. This behavior is a result of the formation of a continuous Al_2O_3 layer on the top surface of the nanostructured HVOF NiCrAlY coating. This layer protects the coating from further oxidation and avoids the formation of mixed oxide protrusions present in the conventional coating.

Introduction

In gas turbine engines, higher efficiency can be achieved by increasing the operating temperature. Hot section components such as combustors, blades and vanes are generally made from nickel-based superalloys such as Inconel 718. The operating temperature of Inconel 718, however, is limited to 650°C, because above this temperature the primary strengthening precipitate ?" particles coarsen rapidly to induce loss in strength [1]. The operating temperature of these metallic components can be increased if a thermal insulation layer is coated on the hot surfaces. A powerful approach to achieve a thermal insulation layer is to apply thermal barrier coatings (TBC) onto the hot surfaces [2-4]. TBCs are capable of increasing the operating temperatures by as much as 200°C [5] and present operating temperatures, for some specific applications, are in the 1000°C range. TBCs also provide protection against high temperature oxidation and hot corrosion attack.

The TBCs applied for Ni super-alloys consist of a ceramic top coat (ZrO_2/Y_2O_3) and a metallic bond coat (MCrAlY, M = Ni, Co or both) [6]. The porous top coat, which is bonded to the bulk material via the bond coat, can protect the underlying air-cooled material by significantly reducing its operating temperature. The metallic bond coat serves also to protect the bulk material from oxidation and corrosion. Conventional commercial MCrAlY coatings have compositions containing: 18-30 wt% Cr, 5-14 wt% Al and balance Ni, Co or Ni and Co in order to provide the best balance between an optimal corrosion protection and a high temperature oxidation [7].

Although the TBC technique was developed for turbine engines over two decades ago, premature failure of TBCs during thermal cycling is still a critical problem, which severely limits the lifetime of the coated components. This premature failure of TBCs is usually caused by the spallation of the top coat, which is mostly due to the thermo-mechanical fatigue cracking along or close to the interface between the bond coat and the top coat [8,9]. The cracking is believed to be related to the thickness and nature of the thermally grown oxide (TGO) layer, which is formed at the interface between the bond coat and the top coat as a result of the reaction between the oxygen penetrating through the top coat and the metallic elements from the bond coat. Therefore, the modification of oxidation behavior in the bond coat is very important in improving the lifetime of TBCs.

In recent efforts to increase the efficiency of gas turbine engines and the lifetimes of high temperature resistant components, the composition of the MCrAlY coatings, together with the variation in grain size, have been studied by Liu *et al*. [10,11]. These researchers have used Magnetron Sputter Deposition (MSD) in order to study the effect of the constituent's composition and grain size on the oxidation behavior of NiCrAl coatings. MSD provides an effective way

of producing fine-grained materials. Their results showed that selective oxidation of Al_2O_3 is a function of the coating grain size and that for the smallest grain size a compact alumina layer was formed on top of the coatings.

For thermal barrier applications, with a typical MCrAlY coating thickness of 100-150 µm, the sputtering technique is economically prohibitive [8,12]. MCrAlY coatings are typically deposited by Vacuum Plasma Spray (VPS), Low Pressure Plasma Spray (LPPS), Atmospheric Plasma Spraying (APS), and recently, High-Velocity Oxy-Fuel spray (HVOF) [11,13]. These techniques can be used for different MCrAlY compositions. However, it is a technological challenge to control the grain size of the coating.

The objectives of the present work are to produce, by the HVOF thermal spray process, a fine-grained coating structure using a nanocrystalline starting powder, and to study the oxidation behavior of these coatings. For comparison reasons, conventional NiCrAlY coatings are also synthesized using the HVOF thermal spray process and the oxidation behavior of these are analyzed as well.

Experimental Procedures

The material system studied in this work was a Ni-22Cr-10Al-1Y (wt%) bond coat deposited on a Ni-based alloy substrate and a Ni alloy foil (ASTM A753-85 alloy type 4) with a thickness of 102 ?m, using the HVOF thermal spray process. The feed stock powder was a commercially available NiCrAlY powder produced by Praxair Surface Technologies - Tafa (Ni-343) with an average particle size of 28 ?m. In order to obtain a nanocrystalline microstructure, the powder was mechanically milled at the rate of 180 rpm in a modified Union Process 01-ST attritor mill for 12 hours under a liquid nitrogen environment. The liquid nitrogen was continuously introduced into the mill during milling to ensure complete immersion of the powders (the process is known as cryomilling or cryogenic milling) [14]. Stainless steel balls with 6.4 mm diameter were used as the grinding media. The ball-to powder weight ratio was 30:1.

A Sulzer Metco Diamond Jet DJ 2700 HVOF thermal spray facility was used for thermal spraying of the NiCrAlY powders. The spraying parameters used to produce the coatings on the Ni based alloy substrates and on the Ni alloy foils are summarized in Table 1. The surface of each substrate was grit blasted before spray. The surface of each foil was not grit blasted, so a flat and smooth surface could be maintained. This type of surface provides poor adherence between the coating and the foil, facilitating the coating removal from the foil after spray. This process results in a free-standing coating.

The number of spraying gun passes can be critical for the oxidation behavior because of the inter-pass oxidation presence in HVOF coatings. To avoid this problem the feed rate and the X-Y transverse speed values for the foil samples were different from the coating samples sprayed on the Ni based substrate. These parameters were chosen so that a thick free-standing coating could be produced with just one pass, avoiding the inter-pass oxidation effect. A detailed schematic of the free-standing sample preparation is shown in Fig. 1. The foil is attached to a steel substrate and it is fixed in place by 2 fixtures. After spray the foil can be easily detached form the coating leaving a free-standing coating sample.

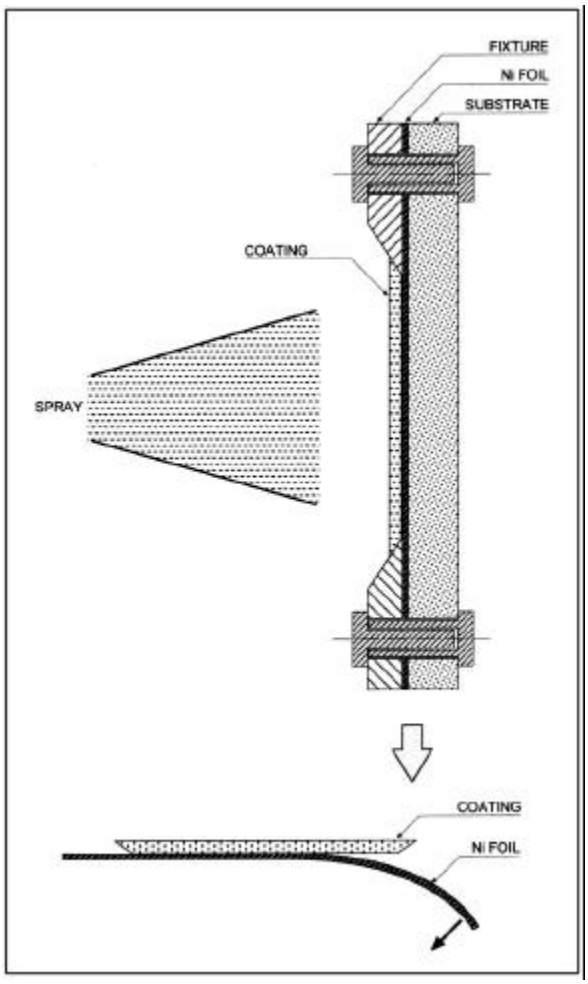

Figure 1. Schematics of the free-standing specimen preparation. The Ni foil is attached to a steel substrate and it is fixed in place by 2 fixtures. After spray the foil can easily be detached from the coating, leaving a free-standing coating sample.

Secondary and backscattered electron images of the coatings were obtained, and EDS analysis was conducted using a Philips XL30 FEG scanning electron microscope (SEM). Samples for SEM observation of the coatings were sectioned from a transverse section and prepared by standard metallographic techniques.

Table 1: Spraying parameters used to produce NiCrAlY coatings.

Gas	Pressure (MPa)	FMR*	GSF**	Parameters	Setting
Air	0.69	40	5616	*Powder feed rate* (Ni based substrate)	0.315 g/s
				Powder feed rate (Ni based foil)	*0.567 g/s*
Fuel (C_3H_6)	0.69	43	1488	X-Y traverse speed (Ni based substrate)	1.10 m/s
				X-Y traverse speed (Ni based foil)	0.55 m/s
O_2	1.034	30	3410	Spraying distance	0.230 m

* FMR = flow meter reading; **GSF: gas standard flow (mm^3/s)

After coating deposition, oxidation experiments were conducted in a high temperature furnace at a constant temperature of 1000°C in air atmosphere for different time periods (4, 12, 24 and 48 hours). Oxidation experiments were conducted on both the coatings deposited on the Ni based substrates and the free-standing coatings, previously removed from the foils. The surfaces, as well as the cross-sections, of the heat-treated coatings were examined using scanning electron microscopy in order to identify phases and morphology of the oxides formed during oxidation. For the free-standing coating, the analysis of the oxidized surface was made on the flat bottom surface, which was in contact with the foil during spraying. This procedure was adopted in order to minimize the effects of surface roughness on the oxide formation.

Results And Discussion

Coating characterization:

The SEM images of the cross-sections of the conventional and nanostructured NiCrAlY coatings obtained using the HVOF thermal spraying process on Ni-based substrates are shown in Fig. 2a and 2b, respectively. In the nanostructured coatings, one can observe a slight increase in porosity when compared to that of the conventional coating. This can be explained by the different agglomerate sizes. After the as received powder was cryomilled, the powder particle or agglomerate experienced a 150% increase in size, even though the material microstructure is reduced to a nanocrystalline regime. Using the same spray conditions for both powders (as received and cryomilled) an increase in porosity content in the coating is expected due to the lack of melting or flattening of the large agglomerates, leaving gaps and voids in the coating.

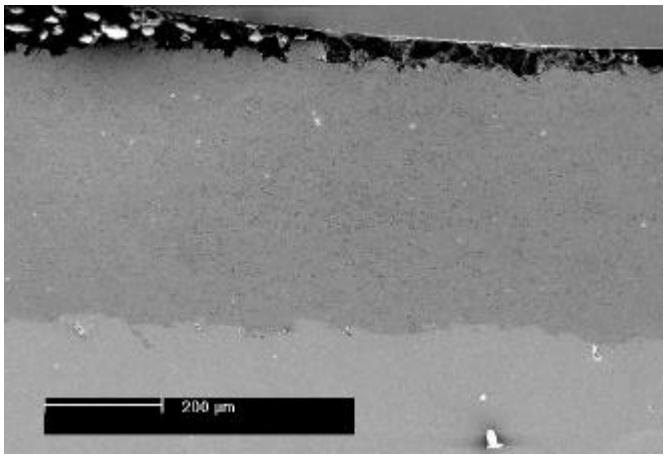

(a)

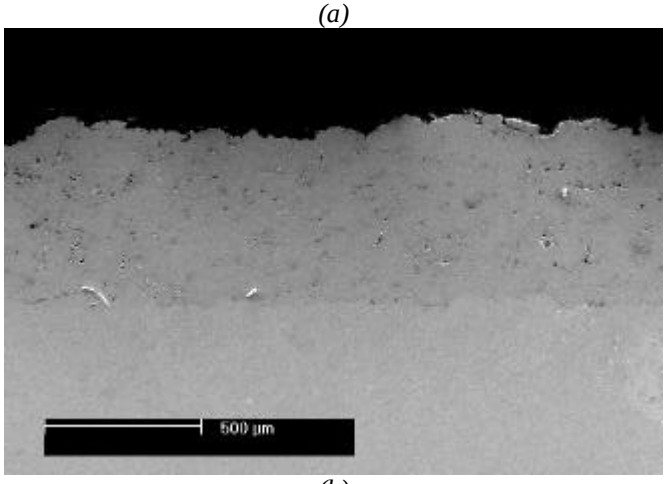

(b)

Figure 2. Cross-section of the (a) conventional and (b) nanostructured NiCrAlY coatings obtained using the HVOF thermal spraying process on Ni-based substrates.

The microstructure of the coatings (conventional and nanocrystalline) are characterized by two phases, ? (Ni, Cr-rich) and ? (Al rich) as shown in Fig. 3 (backscattered electron image of the conventional and the nanocrystalline coating). The bright and dark areas correspond to the ? and ? phases, respectively. According to XRD results, there is also the possibility of ?' phase (Ni_3Al) being present in coating microstructure. The grain size distribution on the conventional coating is relatively homogeneous throughout the cross-section (1-1.5 ?m). The final microstructure of the nanostructured coating has a fine grain structure characterized by a "multimodal structure", in which both nanocrystalline regions (approximately 75 nm (TEM observation [15]) and sub-micron grain regions (from 120 to 550 nm, see Fig. 3) are observed.

In Fig. 4a, one can observe in the backscattered SEM image that there are 4 dark layers in the coating cross-section. According to EDS results, the dark layers are mainly

composed of Al_2O_3, which together with Y_2O_3 are the most kinetically favorable oxide to form. The yttrium content in the alloy is too small to be detected by EDS. This interpass oxidation is a consequence of the high temperature that the coating experienced during the HVOF process. During the time in between passes, the coating surface is still at a high temperature and, in the presence of air, starts to oxidize.

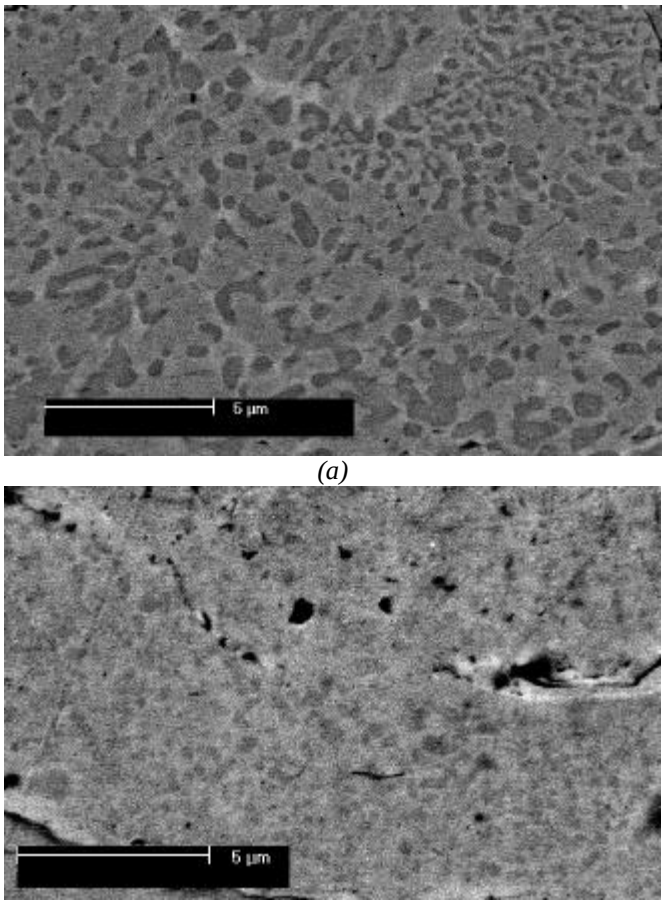

(a)

(b)

Figure 3. SEM image of the cross-section of the (a) conventional and (b) nanostructured NiCrAlY coatings showing the ? and ? phases in the microstructure.

If the same coating is heat treated at a 1000°C for 24 hours a thickening of the interpass oxide layer can be observed (Fig. 4b). This process involves the Al diffusion out of the NiCrAlY alloy and, as a consequence, the development of a NiAl (? phase) depletion zone [16], as observed in Fig. 5. The depletion zone tends to increase in size with the continuation of the oxidation process. The same type of depletion zone is observed immediately below the TGO layer that forms on the top surface of the bond coat.

Oxidation experiments:

For the conventional coatings samples heat treated at 1000°C, the formation of a nonuniform alumina layer can be observed during the first hours of the heat treatment experiments. After the 24h heat treatment, this nonuniform layer manifest itself as mixed-oxide protrusions (Al_2O_3, NiO, and spinel phases like $NiAl_2O_4$ and $NiCr_2O_4$) on top of the initial TGO layer as shown in Fig. 6a. In Fig. 6b one can observe a detailed backscattered image of the mixed oxide layer shown in Fig. 6a. On the basis of their atomic number in the backscattered imaging and EDS analysis, the dark layer close to the coating is Al_2O_3, the intermediate layer is rich in Cr and the upper and brighter layer is rich in Ni.

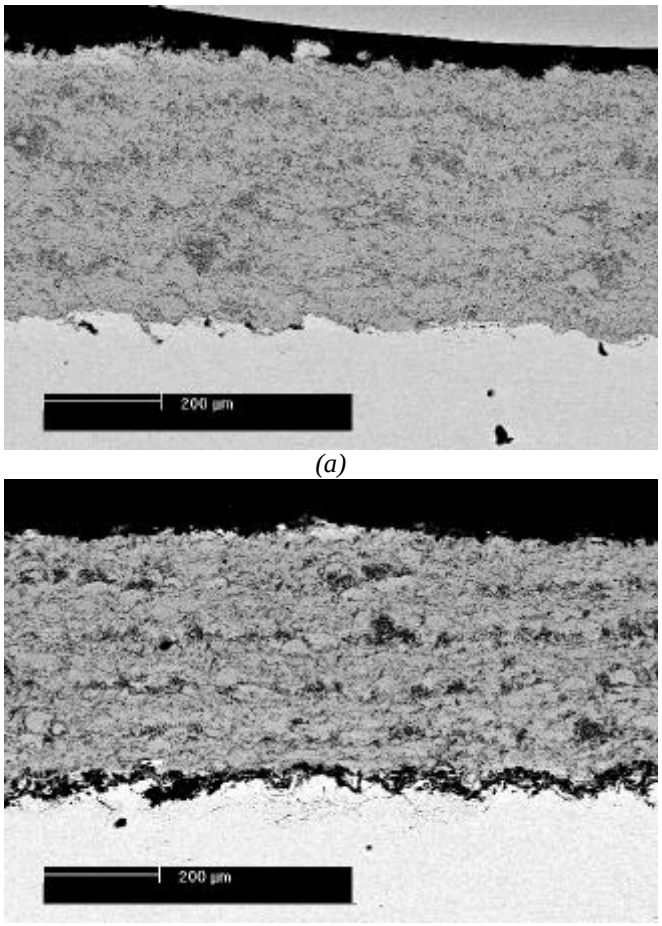

(a)

(b)

Figure 4. (a) SEM image of the cross-section of the conventional NiCrAlY coating showing the interpass oxidation layers after spraying and (b) the same coating after 24 hours at 1000°C.

The morphology and the composition of the top TGO layer are crucial for the performance of TBC coatings. Although the oxidation of Y, Al, and Cr promote a growth in volume of the bond coat, the growth of NiO and spinel phases ($Ni(Cr,Al)_2O_4$) is more damaging because they exhibit a very high growth rate, which rapidly increases the volume of the

bond coat [17] and cause stresses into the YPSZ thermal barrier coating, thus contributing to the initiation of the failure in the TBC system.

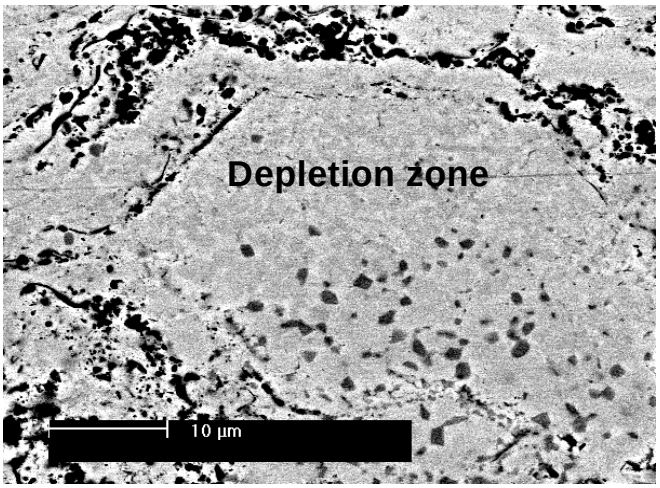

Figure 5. Depletion zone in the conventional HVOF NiCrAlY coating next to an interpass oxide layer after 24 hours at 1000^{o}C heat treatment.

In contrast, for the nanostructured coating one can observe after oxidation (see Fig. 7) the formation of a continuous TGO layer on the coating surface, consisting mainly of Al_2O_3, according to EDS analysis (slow growing oxide [18]). The mixed oxide phases are not observed for the nanocrystalline coating even after 48h at 1000^{o}C. The difference in oxidation behavior can also be observed by viewing the top surface of the free-standing coatings (Fig. 8 and 9).

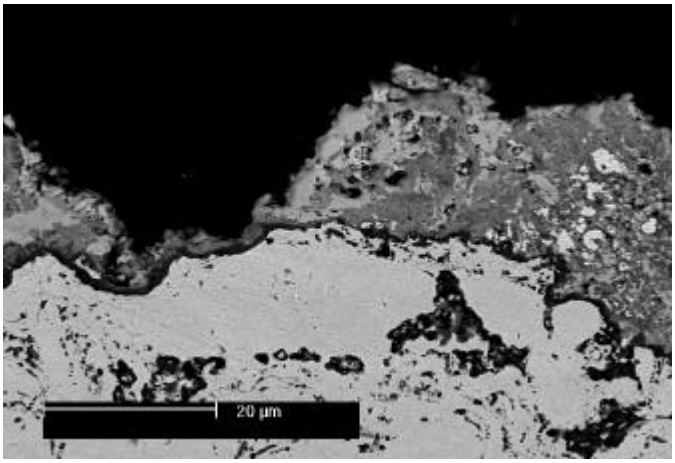

(a)

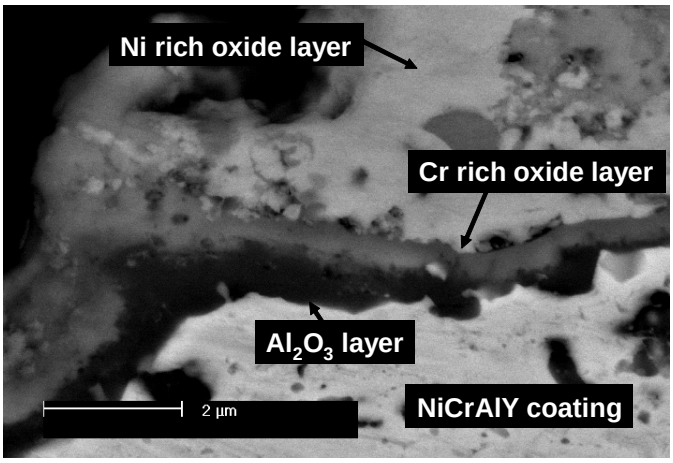

(b)

Figure 6. (a) Formation of the TGO (thermally grown oxide) layer on the surface of the conventional HVOF NiCrAlY coating after heat treatment at 1000^{o}C for 24h. (b) Higher magnification at the interface region.

One advantage of analyzing the free-standing coating (sprayed with just one pass of the spray gun) for the oxidation experiments is the fact that one can isolate the oxidation behavior process without the influence of a depletion zone originated next to an interpass oxide layer. This can be an efficient way to analyze the oxidation behavior of the coating taking into account just it's microstructure, or composition. Another advantage is the fact that one can also isolate the oxidation behavior from the influence of species diffusing from the substrate to the interior of the coating during high temperature experiments.

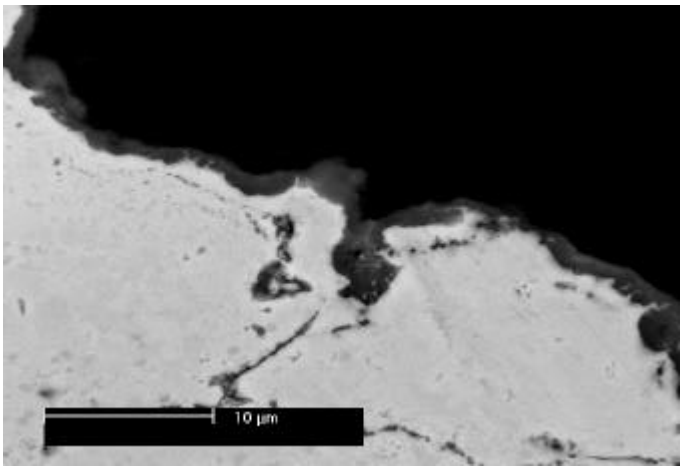

Figure 7. Formation of the TGO (uniform Al_2O_3 layer) on the surface of the nanostructured HVOF NiCrAlY coating after heat treatment at 1000^{0}C for 24h.

The top surface of the conventional free-standing coating oxidized at a 1000^{o}C for 12 hours, seen in Fig. 8a and 8b,

indicates the presence of oxide protrusions and the different morphologies of these constituents. The smoothed ridge structures at lower points of the surface, according to EDS analysis, correspond to the typical Al_2O_3 structure [19], and the polyhedral crystals at higher points on the surface correspond to the NiO structure [17]. The same trend, but with considerable increase in volume, can be observed in Fig. 8c and 8d after 24 hours at the same temperature.

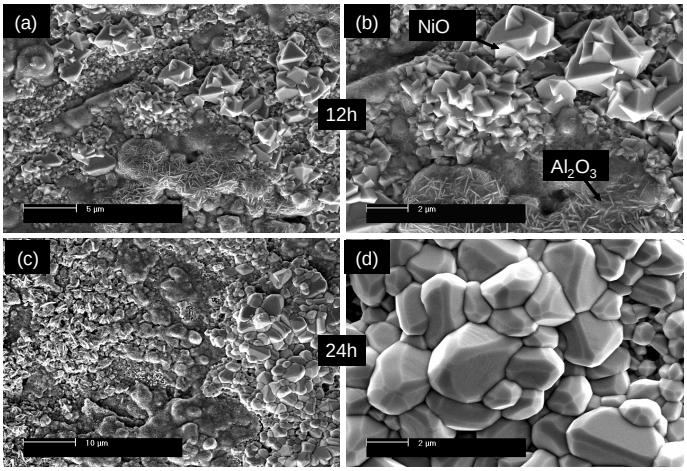

Figure 8. Top surface morphology of the oxide layer on the surface of the conventional free-standing coating ((a) and (b), are oxidized at 1000°C for 12h and (c) and (d) are oxidized at 1000°C for 24h). Mixed oxides are observed at 12h and a considerable increase in oxide volume is observed after 24h. In (d) one can see the coarsening of the NiO crystals with oxidation time.

For the same oxidizing conditions the surface of the nanostructured free-standing coating presented a very different topography than the conventional coating (see Fig. 9). One can see the evolution of oxide scale with time, from 4 to 48 hours of oxidation at 1000°C. From the beginning of the oxidation process, the nanostructured coating presents a uniform and continuous Al_2O_3 layer and the presence of other mixed oxides phases are not observed even for longer oxidation times (48 hours). The transition with time from a morphology of smooth ridges to one with a dense oxide layer can also be observed. Some authors [20] refer to the smooth ridges morphology as characteristic of ?-Al_2O_3, present from the beginning of the oxidation process. Others [21-23], refer to this morphology as characteristic of a meta-stable ?-Al_2O_3 phase that becomes ?-Al_2O_3 with time, changing its morphology from this smooth ridges structure (Fig. 9a to 9d) to an equiaxed grain morphology, as observed in Fig. 9g and 9h. Figure 9e and 9f show the presence of the two morphologies coexisting after 24 hours of oxidation.

The different oxidation behavior is not completely understood and requires further investigation. Nevertheless, a simple experiment was conducted to confirm the importance of the nanocrystalline microstructure on the oxidation behavior of the nanostructured NiCrAlY bond coat. The surface of the oxidized (48h) nanostructured coating was mechanically removed and the sample thickness was reduced by half. The internal microstructure of the coating after 48 hours oxidation was no longer in the nanostructure regime (average grain size = 3.2 ?m). This newly polished surface of the coating was re-oxidized for 12 hours using the same conditions as the previous experiments.

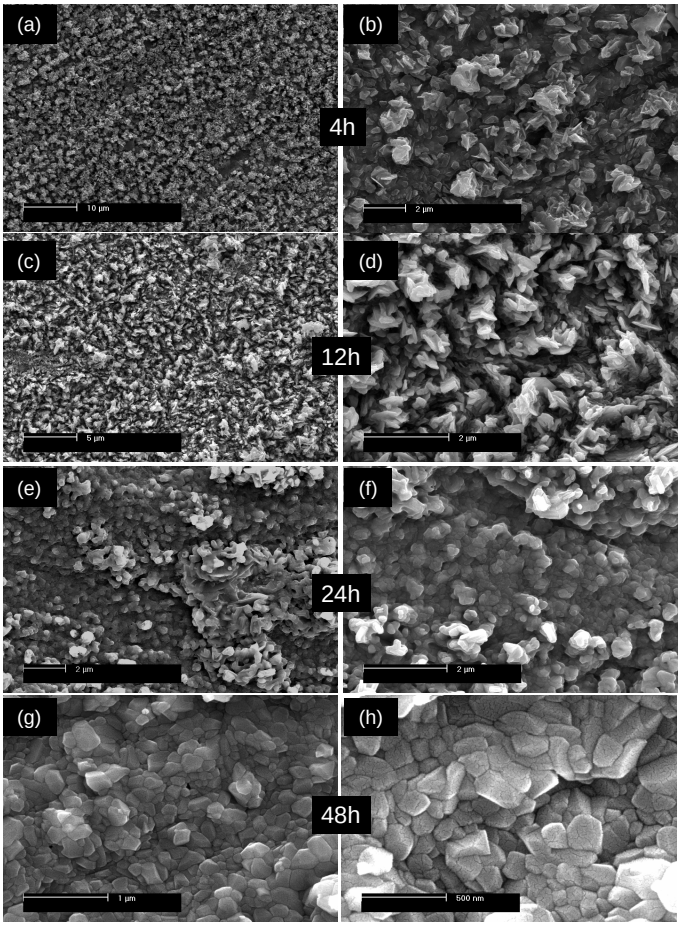

Figure 9. Top surface morphology of the oxide layer at the surface of the nanostructured free-standing coating after oxidation at 1000°C for various times ((a) and (b) 4h; (c) and (d) 12h; (e) and (f) for 24h; and (g) and (h) for 48h). Mixed oxides are not observed. A transition of the Al_2O_3 morphology with time is observed.

As is illustrated in Fig. 10, the new oxide layer formed on the top surface of the re-oxidized sample is composed primary of an Al_2O_3 scale with some small regions where mixed oxide are present. The presence of these different oxides can be explained by observing the cross-section of the coating below these regions (see Fig. 11). Because the sample had already been oxidized for 48 hours prior to the re-oxidation, extensive

inter-lamellar oxidation had occurred; and a depletion zone had formed in the proximity of the inter-lamellar region. Consequently, an insufficient amount of Al atoms remained available for oxidation in these regions, leading to the formation of the mixed oxides regions observed in Fig. 10 and 11.

The fact that a preferential Al_2O_3 oxide layer is observed after the re-oxidation experiment does suggest that the refinement of the microstructure is not the only mechanism responsible for the preferential Al_2O_3 formation on the top surface. The powder exposure to cryommling itself, may modify the coating and influence its oxidation behavior. Cryomilling is known to indtroduce oxides and nitrides finely dispersed within the powders [24]. Further investigation is necessary to fully understand the oxidation mechanism presented in these nanostructured NiCrAlY coatings.

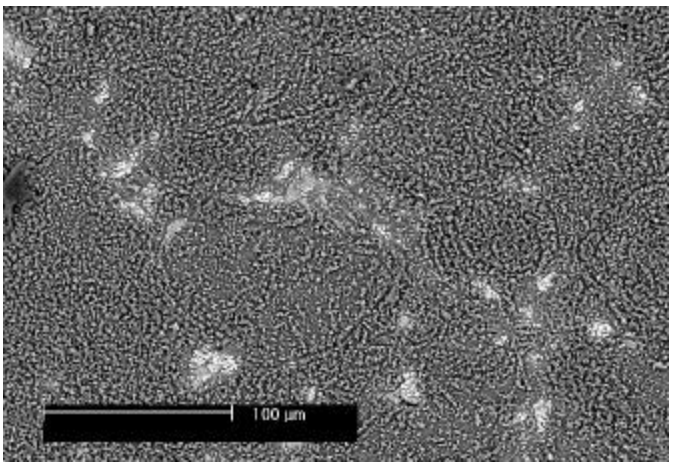

(a)

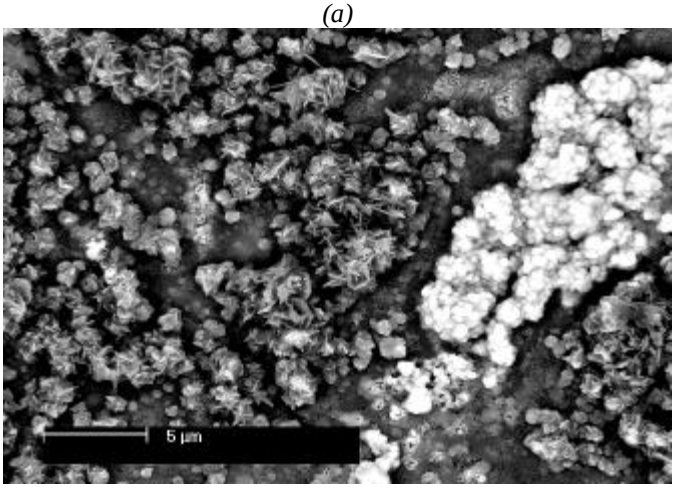

(b)

Figure 10. Re-oxidized nanostructured coating. (a) Top surface showing the dark alumina phase (darker regions) with some small mixed oxides regions (lighter regions). (b) Higher magnification at the interface between the alumina and the mixed oxides regions.

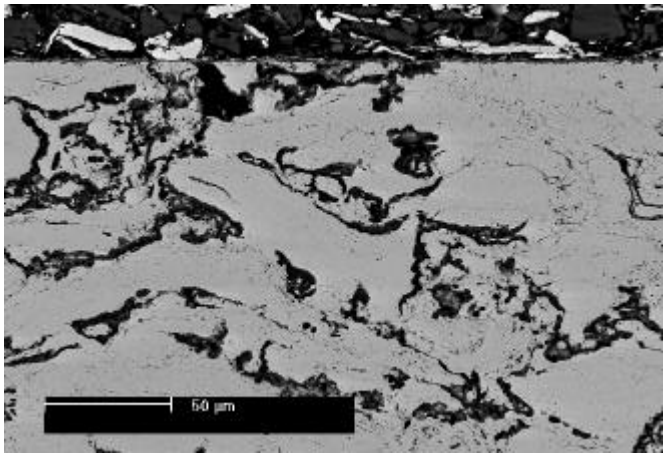

(a)

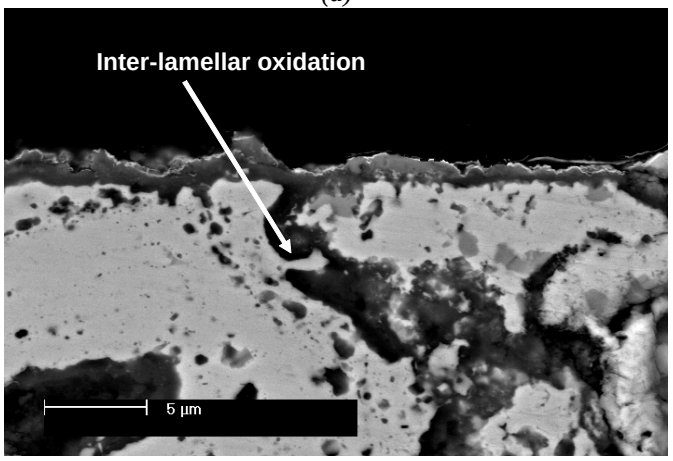

(b)

Figure 11. (a) Cross-section of the re-oxidized nanostructured sample showing severe inter-lamellar oxidation. (b) Higher magnification showing the cross-section beneath the mixed oxide layer.

Summary

The grain size refinement achieved with the cryomilling process was successfully used to produce nanocrystalline NiCrAlY powder and subsequent nanostructured bond coatings using the HVOF thermal spray process.

The oxidation behavior of both conventional and nanostructured NiCrAlY coatings were investigated for heat treatments in air, at 1000^{o}C, for various times. After oxidation, the conventional coating exhibited a discontinuous alumina layer, as well as mixed oxides consisting of and NiO and $Ni(Cr,Al)_2O_4$ spinels. For the nanostructured coating, oxidation led to the formation of continuous alumina layer, without the presence of other mixed oxides.
The difference in oxidation behavior is a direct result of differences in microstructure and phase composition. One or

both of the following mechanisms is influencing the oxidation kinetics. First, the nanocrystalline grain structure results in increased grain boundary area that could enhance aluminum diffusion. Second, the cryomilling introduces finely dispersed oxides that could promote nucleation of alumina. Our work is on-going to identify which of theses mechanisms are, indeed, influencing the oxidation behavior of the NiCrAlY coating.

Aknowledgements

The authors are grateful to the Office of Naval Research (grant N00014-02-1-0213) for their financial support.

References

1. J. He, G. Han, S. Fukuyama and K. Yokogawa, *Acta Mater*., 46, 1998, pp. 215-223.
2. S. Shankar, D. E. Koenig, and L. E. Dardi, *J. Met*., 33, 1981, pp. 13-20.
3. M. A. Gedwill, *NASA TM-81567, National Aeronautics and Space Administration*, Washington, DC, 1980.
4. S. Stecura, *NASA TM-86905, National Aeronautics and Space Administration*, Washington, DC, 1985.
5. H. E. Evans and M. P. Taylor, *Oxidation of Metals*, 55, 2001, pp. 17-34.
6. J.A. Haynes, M.K. Ferber, and W.D. Porter, *J. Thermal Spray Technol.*, 9(1), 2000; pp. 38-48.
7. J.R. Nicholls, N.J. Simms, W.Y Chan and H.E. Evans, *Surf. Coat. Technol.*, 149, 2002, pp. 236-244.
8. R.V. Hillery, B.H. Pilsner, R.L. McKnight, T.S. Cook, M.S. Hartle, *NASA CR 180807, NASA*, Washington, DC, Nov. 1988.
9. Y.H. Sohn, J.H. Kim, E.H. Jordan, and M. Gell, *Surf. Coat. Technol.*, 70, 2001, pp. 146-147.
10. Z. Liu Z., W. Gao, K. Dahm, F. Wang, *Scripta Mater.*, 37(10), 1997, pp. 1551-1558.
11. Z. Liu, W. Gao, K. Dahm, F. Wang, *Acta Mater.*, 46(5) , 1998, pp. 1691-1700.
12 J.T. DeMasi, K.D. Sheffler, S. Bose, *ASME J. of Eng. for Gas Turb. Eng. and Power*, 112, 1990, pp. 521-526.
13. W. Brandl., D. Toma, J. Kruger, H.J. Grabke, G. Matthaus, *Surf. Coat. Technol*., 94-95, 1997, pp. 21-26.
14. H.G. Jiang, M.L. Lau, V.L. Tellkamp, and E.J. Lavernia: *Handbook of Nanostructured Materials and Nanotechnology: Synthesis and Processing*, H. S. Nalwa, Ed., Academic Press, 2000, pp. 159-213.
15. L. Ajdelsztajn, J.A. Picas, G.E. Kim, F. L. Bastian, J. Schoenung, *Mat. Sci. and Eng. A. A* 338, 2002, pp. 33-43.
16. A. Rabiei, A.G. Evans, *Acta Mater*., 48, 2000, pp. 3963-3976.
17. X. Wu, D. Weng, Z. Chen, L. Xu, *Surf. Coat. Tech*., 140, 2001, pp. 231-237.
18. D.F. Susan and A.R. Marder, *Oxidation of Metals*, 75 (1/2), 2002, pp. 159-180.
19. D. Toma, W. Brandl, U. Koster, *Oxidation of Metals*, 53 (1-2), 2000, pp. 125-137.
20. D. Toma, W. Brandl, U. Koster, *Surf. and Coat. Tech*, 120-121, 2000, pp. 8-15.
21. J.C. Yang, E. Schumann, I. Levin, M. Ruhle, *Acta Mater.*, 46, 1998, pp. 2195-2201.
22. G. Muller, G. Schumacher, D. Straub, *Surf. Coat. Tech.*, 108-109, 1998, pp. 43-47.
23. D. Strauss, G. Muller, G. Schumacher, V. Engelko, W. Stamm, D. Clemens, W.J. Quaddakers, *Surf. Coat. Tech*., 135, 2001, pp. 196-201.
24. R. J. Perez, B. Huang and E. J. Lavernia, *Nanostructured Material*, 7, 1996, pp. 565-572.